ISSN 1063-7842, Technical Physics, 2011, Vol. 56, No. 6, pp. 869–876. © Pleiades Publishing, Ltd., 2011.
Original Russian Text © I.A. Lyashenko, 2011, published in Zhurnal Tekhnicheskoĭ Fiziki, 2011, Vol. 81, No. 6, pp. 125–132.

SURFACE, ELECTRON AND ION EMISSION

Tribological System in the Boundary Friction Mode under a Periodic External Action

I. A. Lyashenko

Sumy State University, ul. Rimskogo-Korsakova 2, Sumy, 40007 Ukraine
e-mail: nabla04@ukr.net

Received October 21, 2010

Abstract—A mechanical analog of a tribological system in the boundary friction mode is studied. A thermodynamic model is used to analyze the first-order phase transition between liquidlike and solidlike structures of a lubricant. The time dependences of the friction force, the relative velocity of the interacting surfaces, and the elastic component of the shear stresses appearing in the lubricant are obtained. It is shown that, in the liquidlike state, the shear modulus of the lubricant and the elastic stresses become zero. The intermittent (stick–slip) friction mode detected experimentally is described. It is shown that, as the lubricant temperature increases, the frequency of phase transitions between the lubricant structural states decreases and the total friction force and elastic stress amplitudes lower. When the temperature or the elastic strain exceeds the corresponding critical value, the lubricant melts and a kinetic slip mode in which the elastic component of the friction force is zero takes place.

DOI: 10.1134/S1063784211060168

1. INTRODUCTION

Tribology is part of physics dealing with friction processes, the properties of lubricants, the fracture of interacting surfaces during their relative motion, and so on. In the past two decades, the friction processes at a lubricant thickness less than 10 atomic diameters have been extensively studied owing to the development of high-accuracy experimental techniques [1, 2]. The friction mode that takes place in this situation was called boundary friction, and it frequently occurs in rubbing mechanisms operating under hydrodynamic conditions, where interacting surfaces are in contact because of asperities and heterogeneities [1, 3]. The boundary friction mode differs radically from both dry friction, in which Amonton's law holds true, and fluid (hydrodynamic) friction, where the friction force is proportional to a power function of the velocity. If a lubricant thickness is several atomic layers, we cannot speak about its liquid and solid stable thermodynamic phases [4], since the symmetry of the state depends substantially on the interaction of rubbing surfaces [5]. Therefore, in the boundary friction mode, researchers discuss liquid- and solidlike states of a lubricant, which are interpreted as kinetic friction modes between which first-order phase transitions can occur [6]. These transitions lead an intermittent (stick–slip) character of motion [4, 7].

To study the dynamic characteristics of tribological systems and the rheological properties of lubricants, researchers widely apply molecular dynamics simulation methods [8, 9]. Moreover, phenomenological models are often used, since these methods cannot describe long-term processes because of limited computational abilities of modern computers [5, 7, 10–13]. In particular, in [10, 11], we developed an approach according to which melting of an ultrathin lubricant film between two atomically smooth surfaces proceeds as a result of thermodynamic and shear melting. With this approach, we took into account the effect of the additive noises of basic parameters [14, 15] and correlated temperature fluctuations [16]. It was shown that a self-similar lubricant melting mode takes place at high temperature fluctuation intensities; in this mode, the time series of stresses acquire multifractal properties [17, 18], which are inherent in many systems [19–22]. The causes of the jumplike melting and hysteresis detected experimentally in [2, 23, 24] were considered in [25, 26]. This model was also used to describe a periodic discontinuous friction mode [27, 28].

Popov [5] proposed a thermodynamic theory based on the Landau theory of phase transitions [29] to describe melting of a thin lubricant layer. This model takes into account the loss of shear stability, which leads to a liquidlike structure of a lubricant, due to both thermodynamic melting and the exceeding of the yield strength by stresses (shear melting). The effect of these factors was also studied in [13], where an order parameter was represented by the excess volume [30, 31] induced by the chaotization of the structure of a solid body upon melting. When the excess volume increases, the shear modulus of the lubricant decreases [13]. In [5], an order parameter was chosen to be the shear modulus, which was taken to be zero in a liquidlike phase.

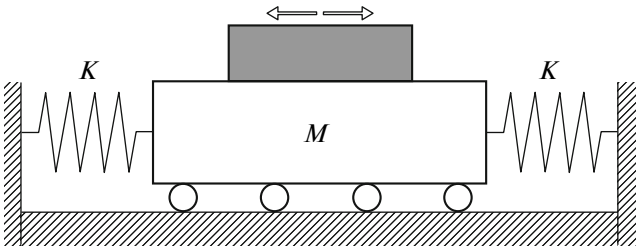

Fig. 1. Schematic diagram of the tribological system.

However, melting of a lubricant in [5] is described as a continuous second-order phase transition, whereas first-order phase transitions [4, 13], which result in discontinuous motion of interacting surfaces [4], often take place in the boundary friction mode. The purpose of this work is to describe the first-order phase transition in a tribological system and to study the lubricant melting kinetics in it in terms of the model from [5].

2. TRIBOLOGICAL SYSTEM

We now consider the tribological system shown in Fig. 1. Here, two springs with stiffness coefficient K are connected to a block of mass M placed on rolls, whose rolling friction is neglected in the further consideration. The second block is situated on this block and is set in motion by external forces. In the presence of interaction forces between the interacting surfaces of these two blocks, the lower block moves when the upper one moves, and the trajectory of the lower block depends strongly on the friction mode. Such a system was studied in [32, 33]. In [32], a steel friction pair is used as an example of interacting surfaces, and ISO 32 paraffinic oil plays the role of a lubricant continuously supplied to the contact zone at a fixed flow rate.

Let X and $V = \dot{X}$ be the upper block coordinate and velocity, respectively, and x and $v = \dot{x}$ be the lower block coordinate and velocity, respectively. We consider the case where the upper block is set in motion according to the cyclic law

$$X = X_m \cos\omega t, \tag{1}$$

$$V = -X_m \omega \sin\omega t, \tag{2}$$

where X_m is the amplitude and ω is the cyclic frequency. The equation of motion of the lower block is written in the form [32]

$$M\ddot{x} + 2Kx - F = 0, \tag{3}$$

where F is the friction force that moves the lower block. Thus, the character of the system motion depends substantially on the friction mode and the properties of the lubricant, since they specify F.

The friction force is determined as the product of the stresses appearing in the lubricant into the contact area of the interacting surfaces A,

$$F = \sigma A. \tag{4}$$

In the boundary friction mode, elastic (σ_{el}) and viscous (dissipative, σ_v) stresses appear in the lubricant layer [5, 13, 24]. Upon melting, the elastic component of the stresses decreases and the viscous component, in contrast, increases due to an increase in the displacement velocity of the interacting surfaces [24]. The total operating stress is the sum of these two contributions,

$$\sigma = \sigma_{el} + \sigma_v. \tag{5}$$

We now determine the viscous stresses in the lubricant layer according to the empirical formula [34]

$$\sigma_v = \frac{\eta_{eff}(V - v)}{h}, \tag{6}$$

where η_{eff} is the effective viscosity of the lubricant and $V - v$ is the relative velocity of the interacting surfaces.

The boundary lubricant represents a non-Newtonian fluid. Such fluids have complex dependences of the viscosity on the velocity gradient. For example, the viscosities of polymer solutions and melts usually decrease with increasing $\dot{\varepsilon}$ (pseudoplastic fluids), and the viscosities of suspensions of solid particles usually, in contrast, increase with $\dot{\varepsilon}$ (dilatant fluids). Therefore, for a qualitative analysis, we use the simple approximation [34]

$$\eta_{eff} = k(\dot{\varepsilon})^{\gamma}, \tag{7}$$

which can take into account both situations. Here, we introduce coefficient of proportionality k [Pa $s^{\gamma+1}$] and dimensionless exponent γ. According to (7), we have $\gamma < 0$ for pseudoplastic fluids, $\gamma > 0$ for dilatant fluids, and $\gamma = 0$ for Newtonian fluids (since the viscosity is velocity-independent here, according to Eq. (7)).

The strain rate is determined through the relative velocity and lubricant thickness h [34],

$$\dot{\varepsilon} = \frac{V - v}{h}. \tag{8}$$

Allowing for Eqs. (7) and (8), we can rewrite Eq. (6) for viscous stresses in the form

$$\sigma_v = k\left(\frac{V - v}{h}\right)^{\gamma+1}. \tag{9}$$

We substitute Eqs. (5) and (9) into Eq. (4) and obtain the following final expression for the friction force [13]:

$$F = \left[\sigma_{el} + k\,\mathrm{sgn}(V - v)\left(\frac{|V - v|}{h}\right)^{\gamma+1}\right]A, \tag{10}$$

where the standard sign function

$$\mathrm{sgn}(V - v) = \begin{cases} 1, & V > v \\ -1, & V < v \end{cases} \tag{11}$$

is introduced to take into account the force direction. Thus, the friction force depends on lower block velocity v and elastic stresses σ_{el} appearing in the lubricant.

3. THERMODYNAMIC MODEL

The free energy density for an ultrathin lubricant layer is written as [5]

$$f = \alpha(T - T_c)\varphi^2 + \frac{a}{2}\varphi^2\varepsilon_{el}^2 - \frac{b}{2}\varphi^4 + \frac{c}{3}\varphi^6 + \frac{g}{2}(\nabla\varphi)^2, \quad (12)$$

where T is the lubricant temperature; T_c is the critical temperature; ε_{el} is the shear component of the elastic strain; α, a, b, c, and g are positive constants; and φ is the order parameter, which is the amplitude of the periodic part of a microscopic function of the medium density [5]. Parameter φ is zero in the liquidlike phase and nonzero in the solidlike phase. As compared to [5, 35], the sign of the third term in potential (12) is changed and the fourth term is added. Such a form of expansion is used to describe first-order phase transitions [29, 35]. Moreover, we introduced factor a into the second term in Eq. (12) to vary the contribution of the elastic energy to the potential.

In [5], squared order parameter φ^2 is numerically equal to shear modulus μ of the lubricant material. As a result, we cannot apply the theory to low-dimensional tribological systems with a lubricant layer of several atomic diameters, since such lubricants can form ordered structures characterized by a high shear modulus (which can be a few orders of magnitude higher than that of the corresponding bulk lubricants [4]) due to compression of the interacting surfaces. In the case of $\mu = \varphi^2$, shear modulus μ cannot have a high value in terms of the model, since expansion (12) holds true in the range $\varphi^2 < 1$.

With Eq. (12), we now specify the elastic stresses as $\sigma_{el} = \partial f/\partial\varepsilon_{el}$,

$$\sigma_{el} = a\varphi^2\varepsilon_{el}. \quad (13)$$

Thus, when introducing coefficient a into expansion (12), we define the shear modulus as

$$\mu = a\varphi^2, \quad (14)$$

and it can acquire high values at low φ. During friction, a lubricant usually melts incompletely when critical temperature T or elastic shear stress σ_{el} is exceeded: a domain structure with fluid and dry friction regions forms. This fact is taken into account in Eq. (12) with the gradient term. The consideration of the domain structure is a separate large problem beyond the scope of this work. Therefore, we will consider the behavior of a lubricant inside one domain with a homogeneous structure and assume $g = 0$.

We now write the following relaxation equation similar to the Landau–Khalatnikov equation [29]:

$$\dot\varphi = -\delta\frac{\partial f}{\partial\varphi}, \quad (15)$$

where δ is the kinetic coefficient characterizing the inertia properties of the system. We substitute energy (12) into Eq. (15) and obtain the equation in an explicit form,

$$\dot\varphi = -\delta(2\alpha(T - T_c)\varphi + a\varphi\varepsilon_{el}^2 - 2b\varphi^3 + 2c\varphi^5) + \xi(t). \quad (16)$$

In (16), we additionally introduced a term that represents additive white noise–type fluctuations with the moments

$$\langle\xi(t)\rangle = 0; \quad \langle\xi(t)\xi(t')\rangle = 2D\delta(t - t'), \quad (17)$$

where D is the stochastic source intensity. When the Eulerian method is used to solve Eq. (16), the corresponding iteration procedure acquires the form [15, 18]

$$\varphi_2 = \varphi_1 - \delta(2\alpha(T - T_c)\varphi + a\varphi\varepsilon_{el}^2 - 2b\varphi^3 + 2c\varphi^5)\Delta t + \sqrt{\Delta t}W_n. \quad (18)$$

Here, Δt is the time integration step and random quantity W_n is introduced. This quantity is defined by the Box–Muller function [18, 36]

$$W_n = \sqrt{2D}\sqrt{-2\ln r_1}\cos(2\pi r_2), \quad r_i \in (0, 1], \quad (19)$$

where r_1 and r_2 are pseudorandom numbers with a uniform distribution. According to the fluctuation-dissipative theorem, additive noise $\xi(t)$ has intensity $D \sim k_B T$, where k_B is the Boltzmann constant. In this case, the fluctuations are too low to change the behavior of the system; however, they should be introduced, since root $\varphi = 0$ in numerical solution of Eq. (16) is stable even if it corresponds to the maximum of potential $f(\varphi)$. If $\xi(t)$ is introduced in this situation, the system passes from an unstable into a stable state, which corresponds to the minimum energy. Thus, fluctuations have to be taken into account because of the specific features of the numerical calculation. In our further calculations, we assume $D = 10^{-25}\ \mathrm{s}^{-1}$.

In a deterministic case, the stationary solution to Eq. (16) has the form

$$\varphi_{1,2}^2 = \frac{b}{2c} \mp \sqrt{\left(\frac{b}{2c}\right)^2 - \left(\frac{a}{2c}\varepsilon_{el}^2 + \frac{\alpha(T - T_c)}{c}\right)}, \quad (20)$$

where sign "–" corresponds to an unstable solution with symmetric potential maxima and sign "+" corresponds to a stable solution with the minimum energy.

Figure 2 shows the stationary values of the squared order parameter calculated by Eq. (20) at fixed values of the elastic strain (Fig. 2a) and the lubricant temperature (Fig. 2b). Solid segments of the curves correspond to stable stationary solutions, and dashed segments correspond to unstable solutions.

At a zero elastic strain and low temperature T, the lubricant is solidlike, since parameter φ is nonzero and, according to Eq. (14), shear modulus μ is also nonzero (Fig. 2a, continuous section of curve *1*). In this case, potential (12) has two symmetric minima separated by a zero maximum. When the critical temperature

$$T_{c0} = T_c - \frac{a}{2\alpha}\varepsilon_{el}^2 + \frac{b^2}{4\alpha c} \quad (21)$$

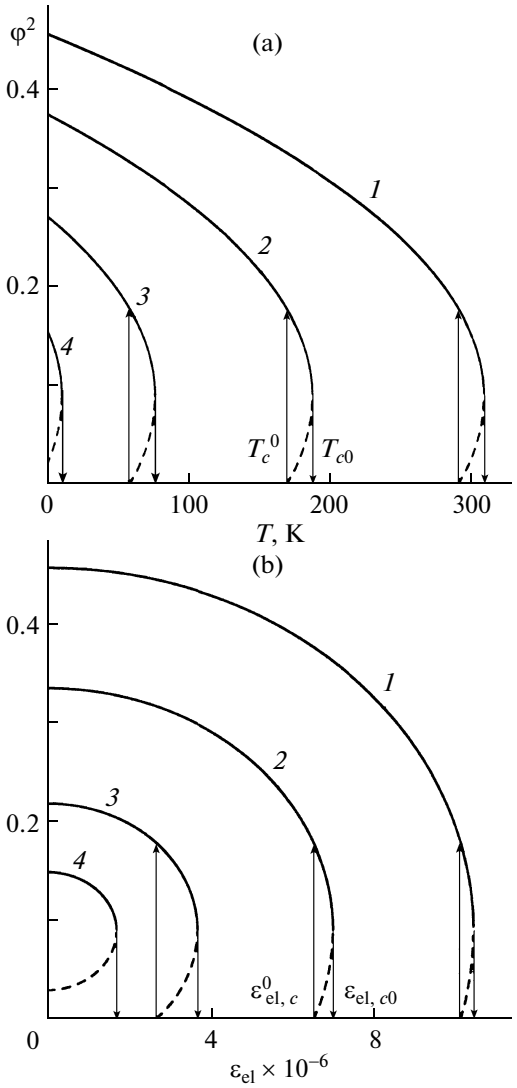

Fig. 2. Stationary values of squared order parameter φ^2 (dimensionless quantity) vs. lubricant temperature T and elastic component of strain ε_{el} (dimensionless quantity) at $\alpha = 0.7$ J K^{-1}/m^3, $T_c = 290$ K, $a = 4 \times 10^{12}$ Pa, $b = 285$ J/m^3, and $c = 1600$ J/m^3 (see Eq. (20)): (a) curves *1–4* correspond to fixed strains $\varepsilon_{el} = 0$, 6.5×10^{-6}, 9×10^{-6}, and 10.2×10^{-6}, respectively; (b) curves *1–4* are plotted at fixed temperatures $T = 0$, 170, 270, and 300 K, respectively.

is exceeded, the squared order parameter changes jumpwise to a zero value and the lubricant changes into a liquidlike state, where potential $f(\varphi)$ has a single zero minimum. If T is decreased after this transition, the lubricant solidifies at a lower temperature,

$$T_c^0 = T_c - \frac{a}{2\alpha}\varepsilon_{el}^2, \tag{22}$$

and the squared order parameter again becomes nonzero. In the intermediate range $T_c^0 < T < T_{c0}$, the potential is characterized by two symmetric minima (solid segment of the curve) separated by symmetric maxima (dashed segment) from a zero minimum. Thus, dependence $\varphi^2(T)$ has a hysteretic character and corresponds to a first-order phase transition. According to Fig. 2a, the lubricant melts at a lower temperature when the elastic strain increases. Curve *4* corresponds to the situation where the lubricant cannot solidify after melting due to a decrease in the temperature.[1] When the strain increases further above a certain critical value, the lubricant is always liquidlike ($\mu = 0$) irrespective of the temperature.[2]

According to Fig. 2b, the lubricant melts when the strain exceeds

$$\varepsilon_{el,c0} = \sqrt{\frac{2\alpha(T_c - T)}{a} + \frac{b^2}{2ac}} \tag{23}$$

and the lubricant solidifies when ε_{el} becomes lower than

$$\varepsilon_{el,c}^2 = \sqrt{\frac{2\alpha(T_c - T)}{a}}. \tag{24}$$

Here, the situation is analogous to that shown in Fig. 2a. Thus, melting occurs due to both an increase in temperature T and a mechanical action with increasing strain ε_{el}; that is, the model takes into account thermodynamic and shear melting.

In experiments, the shear velocity rather than the shear component of the strain (ε_{el}) is usually detected. Therefore, we need a relation between these quantities to perform a further investigation. To this end, we use the Debye approximation, which relates elastic component of strain ε_{el} to plastic component ε_{pl} [5],

$$\dot{\varepsilon}_{pl} = \frac{\varepsilon_{el}}{\tau_\varepsilon}, \tag{25}$$

where τ_ε is the Maxwell time of relaxation of internal stresses. The total strain in the layer is determined by the sum of the elastic and plastic components [5, 31],

$$\varepsilon = \varepsilon_{el} + \varepsilon_{pl}. \tag{26}$$

When combining Eqs. (8), (25), and (26), we obtain an expression for the elastic component of the shear strain [13],

$$\tau_\varepsilon \dot{\varepsilon}_{el} = -\varepsilon_{el} + \frac{(V - v)\tau_\varepsilon}{h}. \tag{27}$$

4. MELTING KINETICS

The dynamic characteristics of any tribological system are determined by its general properties. For example, the behavior of a system in the situation shown in Fig. 1 depends substantially on the stiffness coefficient of the springs and the lower block mass. In

[1] The corresponding critical strain can easily be found from Eq. (22) at $T_c^0 = 0$ or from Eq. (24) at $T = 0$.

[2] The corresponding critical strain is determined from Eq. (21) at $T_{c0} = 0$ or from Eq. (23) at $T = 0$.

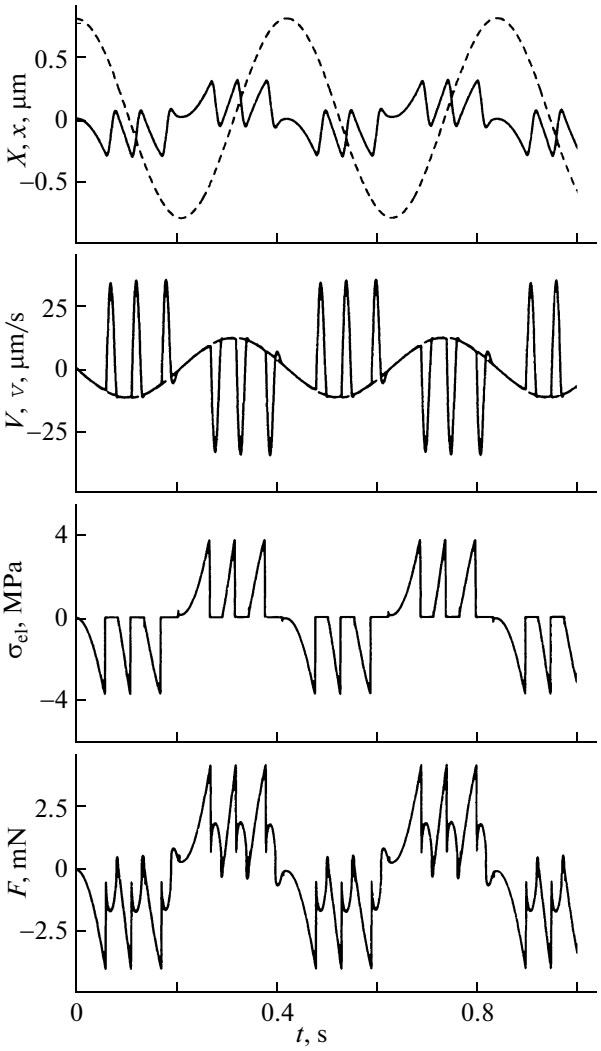

Fig. 3. Dependences of coordinates X, x; velocities V, v; elastic stresses σ_{el} (Eq. (13)); and friction force F (Eq. (10)) on time t at the parameters of Fig. 2 and $h = 10^{-9}$ m, $\tau_\varepsilon = 10^{-8}$ s, $\gamma = -2/3$, $A = 10^{-9}$ m^2, $k = 5 \times 10^4$ Pa s$^{1/3}$, $\delta = 100$ J^{-1} m^3/s, $T = 220$ K, $X_m = 8 \times 10^{-5}$ m, $\omega = 15$ rad/s, $M = 0.4$ kg, and $K = 7000$ N/m. (Dashed lines) $X(t)$ and $V(t)$, (solid lines) $x(t)$ and $v(t)$.

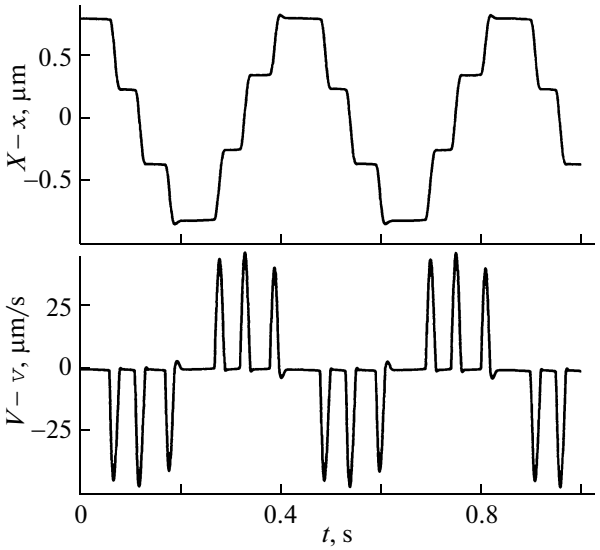

Fig. 4. Dependences of relative displacement $X(t) - x(t)$ and relative velocity $V(t) - v(t)$ of the rubbing blocks on time t that correspond to the curves in Fig. 3.

contrast to motion with constant elastic strains (see Fig. 1), a stick–slip motion mode can occur in such a tribological system during friction [4, 7, 27]. This mode is caused by the fact that a lubricant melts and solidifies periodically during motion, which results in an oscillating character of friction force F.

To calculate the time evolution of the system, we have to simultaneously solve kinetic equations (3), (16), and (27) by determining friction force F from Eqs. (10) and (11) and elastic stresses σ_{el} from Eq. (13). In solving these equations, we should take into account the relation $\dot{x} = v$ and Eqs. (1) and (2). Since strain relaxation time τ_ε is small, we simultaneously solve Eqs. (3) and (16) and determine the current strain from the relationship

$$\varepsilon_{el} = \frac{(V - v)\tau_\varepsilon}{h}, \qquad (28)$$

which follows from Eq. (27) according to the adiabatic approximation $\tau_\varepsilon \dot{\varepsilon}_{el} \approx 0$. Hereafter, the time integration step is chosen to be $\Delta t = 10^{-10}$ s for a numerical analysis.

Figure 3 shows the results of solving these equations. The dashed line in the upper panel shows the $X(t)$ dependence of the upper block coordinate (see Eq. (1)), and the solid line illustrates lower block coordinate $x(t)$, which has a more complex time dependence. Figure 3 also depicts the time dependences of the block velocities, elastic shear stresses σ_{el} (Eq. (13)) appearing in the lubricant, and total friction force F (Eq. (10)). At time $t = 0$, the rubbing blocks are at rest and the lubricant is solidlike, since its temperature is $T < T_c$ and $\varepsilon_{el} = 0$ at rest. At $t > 0$, the upper block begins to move and its velocity increases according to Eq. (2).

Since the lubricant is solidlike, friction force F has viscous and elastic components and the lower block is entrained by the upper block. However, when the lower block moves, the absolute value of elastic force Kx, which hinders the motion of the lower block, increases. As a result, lower block velocity v increases more slowly than V. In this case, the relative displacement velocity of the interacting surfaces $V - v$ increases, condition (23) is met at a certain time, and the lubricant melts. The friction force decreases substantially, since the stresses become zero, and the lower block slips over a significant distance due to the

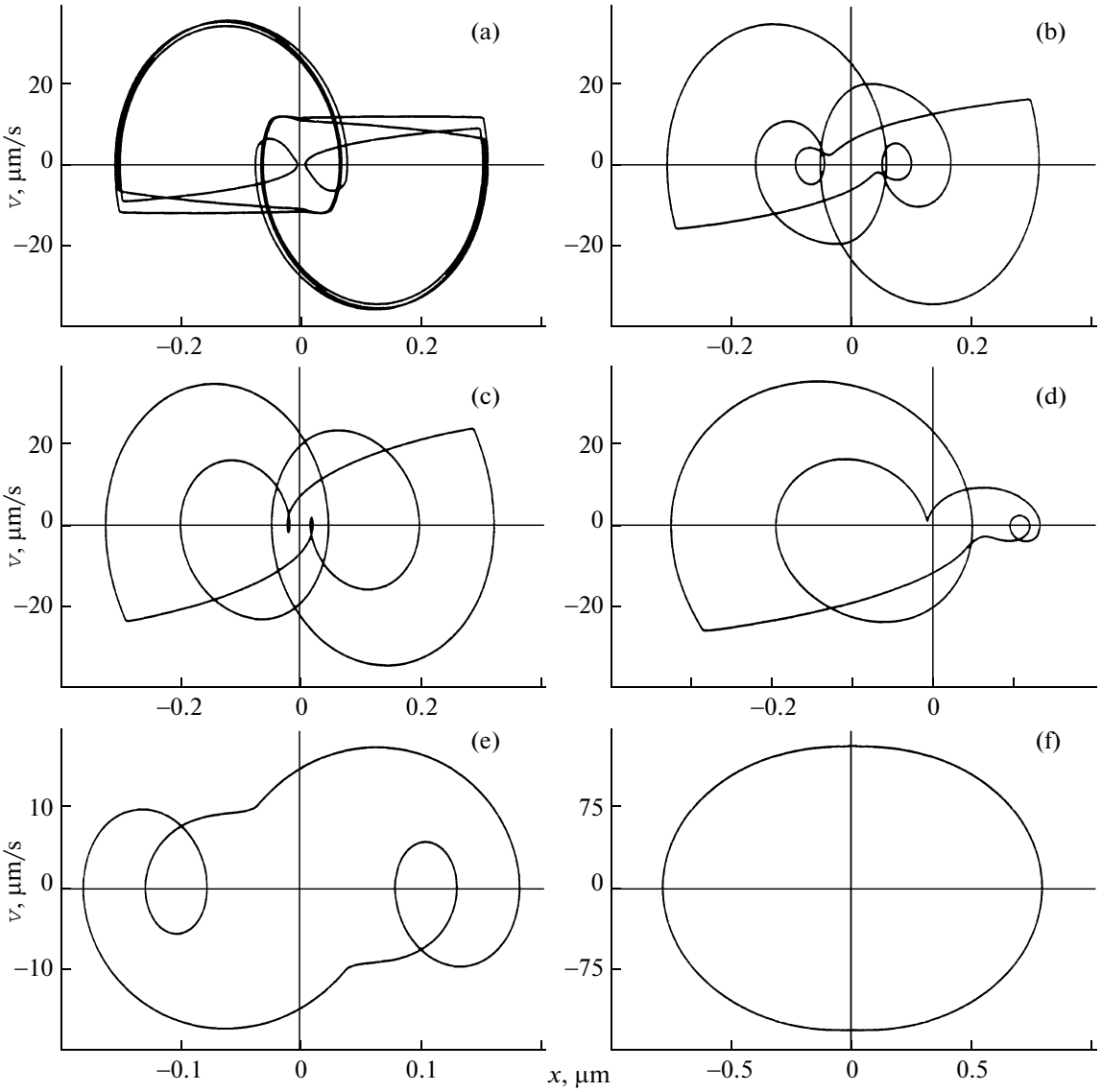

Fig. 5. Phase portraits $\dot{x}(x)$ of the system corresponding to the parameters in Fig. 4 and frequencies ω = (a) 15, (b) 25, (c) 38, (d) 40, (e) 50, and (f) 170 rad/s.

elastic force created by the compressed and tensioned springs. As a result, the relative displacement velocity decreases and the lubricant again solidifies when condition (24) is met. This process is periodic in time.

Figure 4 shows the time dependences of the relative motion of the blocks and their relative velocity. At the times when the surfaces "stick," relative displacement $X - x$ remains constant and relative displacement velocity $V - v$ is close to zero ($V(t)$ and $v(t)$ dependences in Fig. 3 coincide visually). Thus, a periodic stick–slip motion mode, which is also characteristic of dry friction without a lubricant [1, 37], takes place. At the chosen parameters for one full period, the blocks stick six times to each other, i.e., three times for motion in each direction, and these dependences are symmetric with respect to the motion direction. However, different situations can occur depending on the parameters.

The phase portraits of the system at the parameters of Fig. 4 and various values of cyclic frequency ω are presented in Fig. 5. It is clearly visible that the behavior of the system becomes simpler with increasing frequency, since the total number of harmonics decreases. Note that all phase portraits are symmetric with respect to the origin of coordinates apart from the portrait in Fig. 5d, which demonstrates the situation where the motion of the upper interacting surface in both directions differently affects the motion of the lower surface. This case corresponds to memory effects detected experimentally in the system [4]. Since this situation differs radically from other ones, we additionally show the time dependences of the

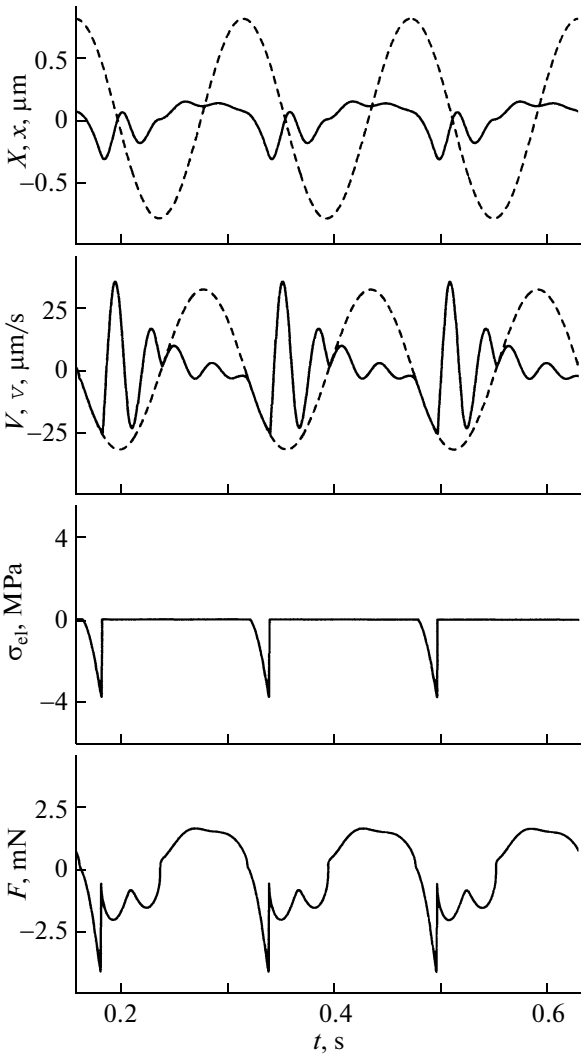

Fig. 6. Time dependences of the quantities corresponding to the parameters in Fig. 5d.

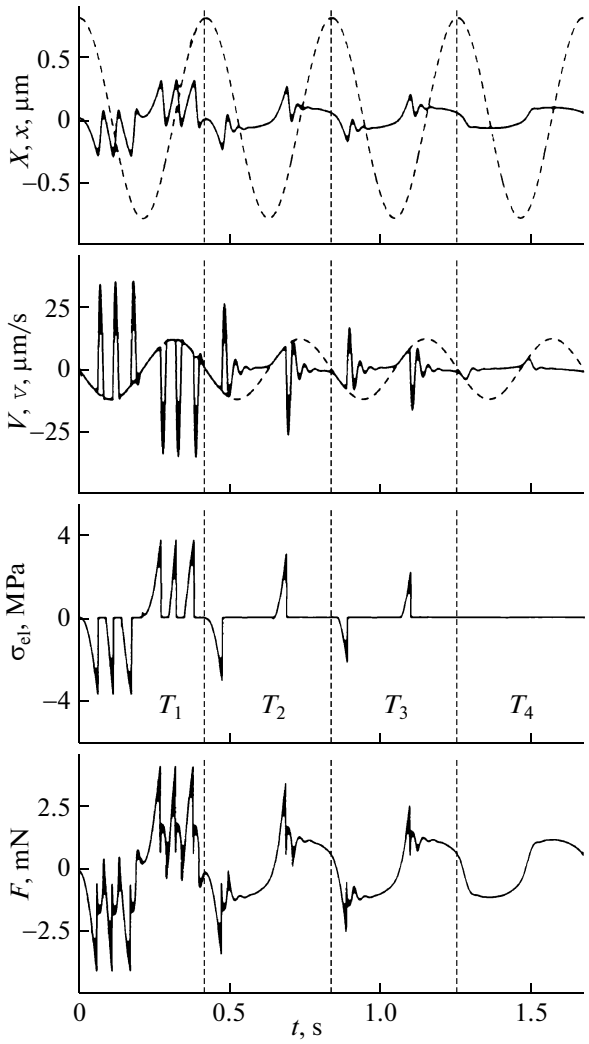

Fig. 7. Dependences of coordinates X, x; velocities V, v; elastic stresses σ_{el} (Eq. (13)); and friction force F (Eq. (10)) on time t at the parameters of Fig. 3 and temperatures $T_1 =$ 220 K, $T_2 = 240$ K, $T_3 = 265$ K, and $T_4 = 280$ K. (Dashed lines) $X(t)$ and $V(t)$, (solid lines) $x(t)$ and $v(t)$.

quantities under study in Fig. 6 for this situation. According to these dependences, the motion of the lower block is also periodic in time; however, the times of sticking of the surfaces take place when the upper block moves in one direction at positive X and $V < 0$. At a frequency $\omega = 170$ rad/s (Fig. 5f), Eq. (2) demonstrates that the displacement velocity is such that the lubricant is always liquidlike; therefore, the corresponding phase portrait reflects periodic motion according to a law similar to Eq. (1). Note that the phase portrait in Fig. 5a is plotted at a frequency $\omega =$ 15 rad/s, which corresponds to the time dependences given in Fig. 3.

Figure 7 corresponds to an increase in lubricant temperature T. Here, the dependences are divided into four sections in the time axis such that the temperature of the next section is higher than that of the previous one. The dependence in the first section ($T = T_1$) repeats the dependence shown in detail in Fig. 3, since it was obtained at the same lubricant temperature. When the temperature increases ($T = T_2$), the stick–slip motion mode takes place, as in the case of $T = T_1$; however, the number of stick peaks decreases and they become lower. In other words, the friction force in the solidlike state of the lubricant decreases with increasing temperature, and the lubricant is in a liquidlike state for a longer time in the period. As the temperature increases further ($T = T_3$), the elastic stress and friction force amplitudes become lower. At $T = T_4$, the lubricant is liquidlike and the elastic stresses are zero. To the best of our knowledge, there are no experiments in which the effect of temperature was studied; therefore, the dependences shown in Fig. 7 are predictive.

5. CONCLUSIONS

We proposed a theoretical model based on the existing thermodynamic model in order to explain a number of effects appearing in the boundary friction mode. This stick-slip friction mode was shown to be caused by a first-order phase transition between liquidlike and solidlike structures of a lubricant. When studying the effect of temperature on melting, we found that, as the temperature increases, the lubricant melts at lower relative displacement velocities of the interacting surfaces. We revealed a mode in which the displacement of the interacting surfaces is not equivalent with respect to the motion direction of the upper interacting surface.

To develop the model, we used a symmetric thermodynamic potential having one zero maximum and two nonzero minima symmetric with respect to this zero maximum (they correspond to equivalent states of the lubricant). However, it was experimentally detected that boundary lubricants are characterized by more than one type of transition and can exist in more than two (solidlike, liquidlike) metastable states. To describe this situation, it is sufficient to take into account additional expansion terms of higher orders in the potential. Since the model is quantitative, its modifications can be used to describe specific experiments.

REFERENCES

1. B. N. J. Persson, *Sliding Friction: Physical Principles and Applications* (Springer, New York, 2000).
2. J. Israelachvili, Surf. Sci. Rep. **14**, 109 (1992).
3. J. Ringlein and M. O. Robbins, Am. J. Phys. **72**, 884 (2004).
4. H. Yoshizawa and J. Israelachvili, J. Phys. Chem. **97**, 11300 (1993).
5. V. L. Popov, Zh. Tekh. Fiz. **71** (5), 100 (2001) [Tech. Phys. **46**, 605 (2001)].
6. E. A. Brener and V. I. Marchenko, Pis'ma Zh. Eksp. Teor. Fiz. **76**, 246 (2002) [JETP Lett. **76**, 211 (2002)].
7. A. E. Filippov, J. Klafter, and M. Urbakh, Phys. Rev. Lett. **92**, 135503 (2004).
8. O. M. Braun and A. G. Naumovets, Surf. Sci. Rep. **60**, 79 (2006).
9. P. A. Thompsom and M. O. Robbins, Science **250**, 792 (1990).
10. A. V. Khomenko and O. V. Yushchenko, Phys. Rev. E **68**, 036110 (2003).
11. A. V. Khomenko and I. A. Lyashenko, Condens. Matter. Phys. **9**, 695 (2006).
12. J. M. Carlson and A. A. Batista, Phys. Rev. E **53**, 4153 (1996).
13. I. A. Lyashenko, A. V. Khomenko, and L. S. Metlov, Zh. Tekh. Fiz. **80** (8), 120 (2010) [Tech. Phys. **55**, 1193 (2010)].
14. A. V. Khomenko and I. A. Lyashenko, Zh. Tekh. Fiz. **75** (11), 17 (2005) [Tech. Phys. **50**, 1408 (2005)].
15. A. V. Khomenko and I. A. Lyashenko, Zh. Tekh. Fiz. **77** (9), 137 (2007) [Tech. Phys. **52**, 1239 (2007)].
16. A. V. Khomenko and I. A. Lyashenko, Fluct. Noise Lett. **7**, L111 (2007).
17. A. V. Khomenko, I. A. Lyashenko, and V. N. Borisyuk, Ukr. Fiz. Zh. **54**, 1142 (2009).
18. A. V. Khomenko, I. A. Lyashenko, and V. N. Borisyuk, Fluct. Noise Lett. **9**, 19 (2010).
19. A. Carpinteri, A. Spagnoli, and S. Vantadori, Fatigue Fract. Eng. Mater. Struct. **25**, 619 (2002).
20. A. Carpinteri, A. Spagnoli, and S. Vantadori, Int. J. Fatigue **31**, 927 (2009).
21. A. Carpinteri and A. Spagnoli, Int. J. Fatugue **26**, 125 (2004).
22. A. Carpinteri, A. Spagnoli, and S. Vantadori, Eng. Fract. Mech. **77**, 974 (2010).
23. A. L. Demirel and S. Granick, J. Chem. Phys. **109**, 6889 (1998).
24. G. Reiter, A. L. Demirel, J. Peanasky, L. L. Cai, and S. Granick, J. Chem. Phys. **101**, 2606 (1994).
25. A. V. Khomenko and I. A. Lyashenko, Fiz. Tverd. Tela (St. Petersburg) **49**, 886 (2007) [Phys. Solid State **49**, 936 (2007)].
26. A. V. Khomenko and I. A. Lyashenko, Phys. Lett. A **366**, 165 (2007).
27. A. V. Khomenko and I. A. Lyashenko, Zh. Tekh. Fiz. **80** (1), 27 (2010) [Tech. Phys. **55**, 26 (2010)].
28. A. V. Khomenko and I. A. Lyashenko, Trenie Iznos **31**, 412 (2010).
29. L. D. Landau and E. M. Lifshitz, *Course of Theoretical Physics*, Vol. 5: *Statistical Physics* (Nauka, Moscow, 1995; Pergamon, Oxford, 1980), Part 1.
30. A. Lemaitre and J. Carlson, Phys. Rev. E **69**, 061611 (2004).
31. A. Lemaitre, Phys. Rev. Lett. **89**, 195503 (2002).
32. C.-R. Yang, Y.-C. Chiou, and R.-T. Lee, Tribol. Int. **32**, 443 (1999).
33. C.-R. Yang, R.-T. Lee, and Y.-C. Chiou, Tribol. Int. **30**, 719 (1997).
34. G. Luengo, J. Israelachvili, and S. Granick, Wear **200**, 328 (1996).
35. V. L. Popov, Pis'ma Zh Tekh. Fiz. **25** (20), 31 (1999) [Tech. Phys. Lett. **25**, (10) 815 (1999)].
36. W. H. Press, B. P. Flannery, S. A. Teukolsky, and W. T. Vetterling, *Numerical Recipes in C: The Art of Scientific Computing*, 2nd ed. (Cambridge Univ., New York, 1992).
37. I. A. Lyashenko, Zh. Tekh. Fiz. **81** (5), 115 (2011) [Tech. Phys. **56**, 701 (2011)].

Translated by K. Shakhlevich